SUPPLEMENTAL MATERIAL

Wu et al., https://doi.org/10.1084/jem.20171341

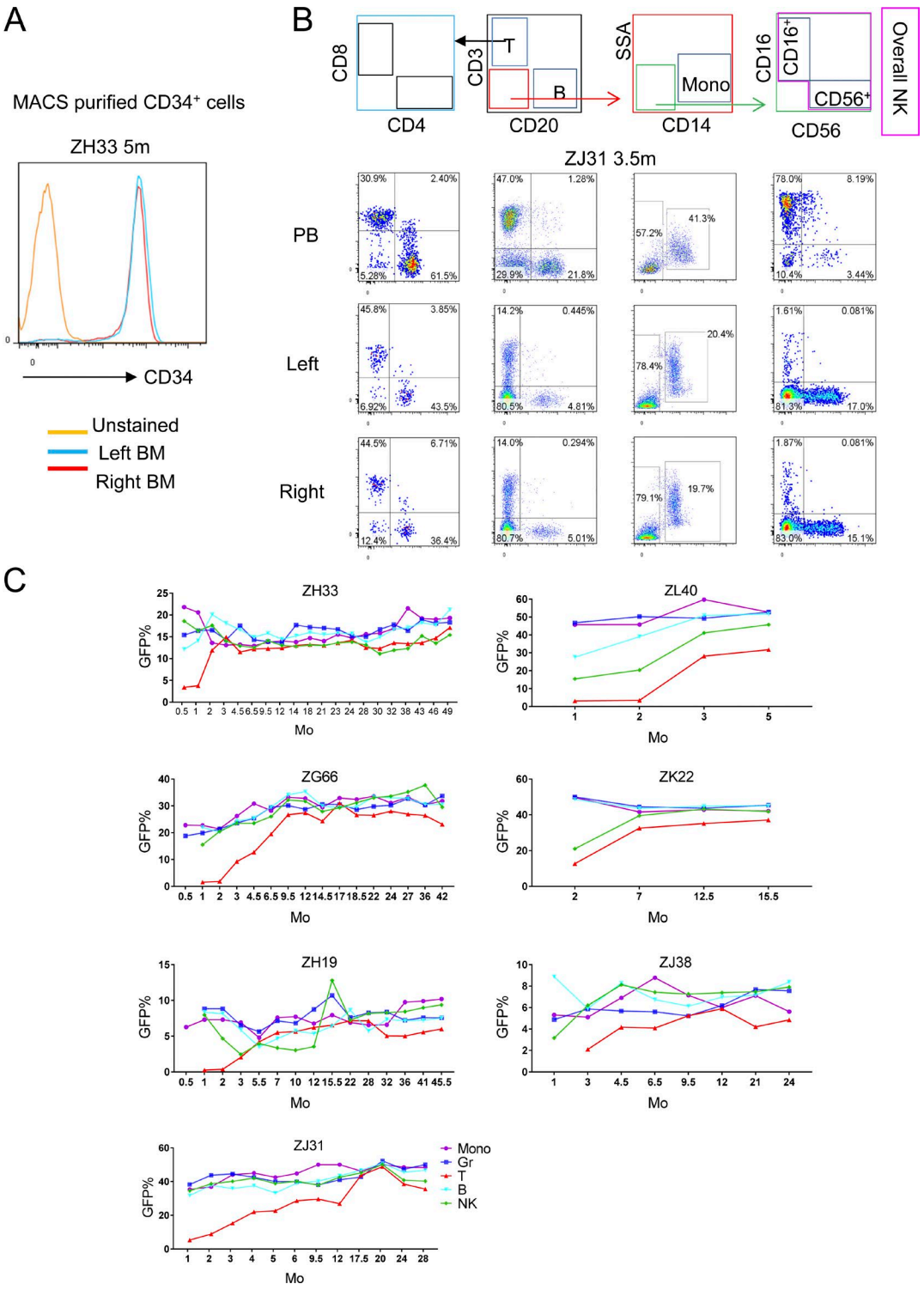

Figure S1. **Purification strategies for HSPCs and specific hematopoietic lineages and GFP marking for PB lineages. (A)** Representative flow cytometric analysis of BM CD34⁺ HSPCs from rhesus macaque ZH33 5 mo after transplantation, purified using MACS bead immunoselection. **(B)** Top: Schematic of flow cytometric gating strategy used for sorting lineage-specific cells from the PB or BM of rhesus macaques. Bottom: Flow cytometry plots for a representative set of concurrent PB and both left and right BM samples stained and gated as shown in the schematic. Samples obtained from rhesus macaque ZJ31 3.5 mo after transplantation. The percentages of the gated cells are displayed on the plots. **(C)** Percentage of GFP-positive cells (reflecting percentage of cells containing the barcode) over time in PB T, B, Mono, Gr, and NK cells (including both CD56⁺/CD16⁻ and CD56⁻/CD16⁺ NK cells) over time after transplantation in seven animals.

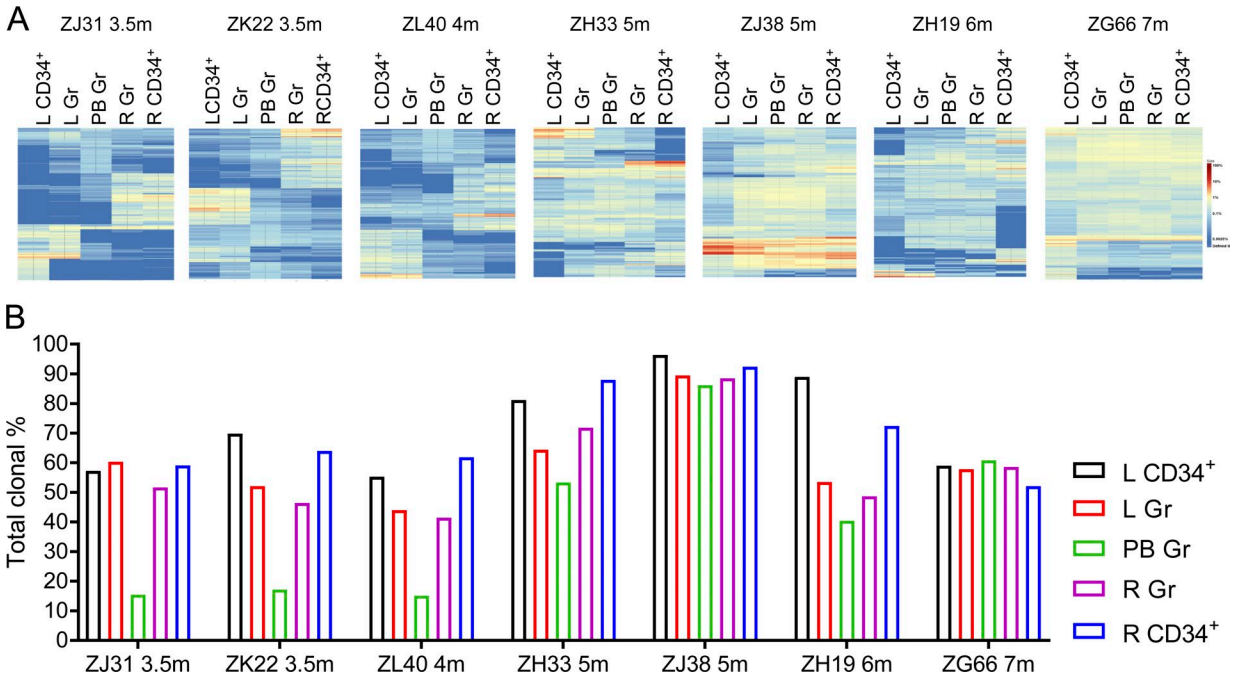

Figure S2. **Clonal patterns of top 100 high-contributing clones from left versus right BM CD34⁺ HSPCs and Gr from BM and PB at 3.5–7 mo posttransplantation. (A)** Heat maps represent log fractional contributions of the top 100 most abundant clones in a sample mapped over all samples. Each row corresponds to one barcode, and each column to a sample. Each * designates that the barcode is one of the top 100 barcodes in that sample. The top 100 clones in each sample are plotted across all samples, so each row in the heat map has at least one *, and each column has exactly 100 *. The barcodes are ordered by unsupervised hierarchical clustering using Euclidean distances. **(B)** The fraction of total barcode abundance in the sample contributed by the clones mapped in each column of A.

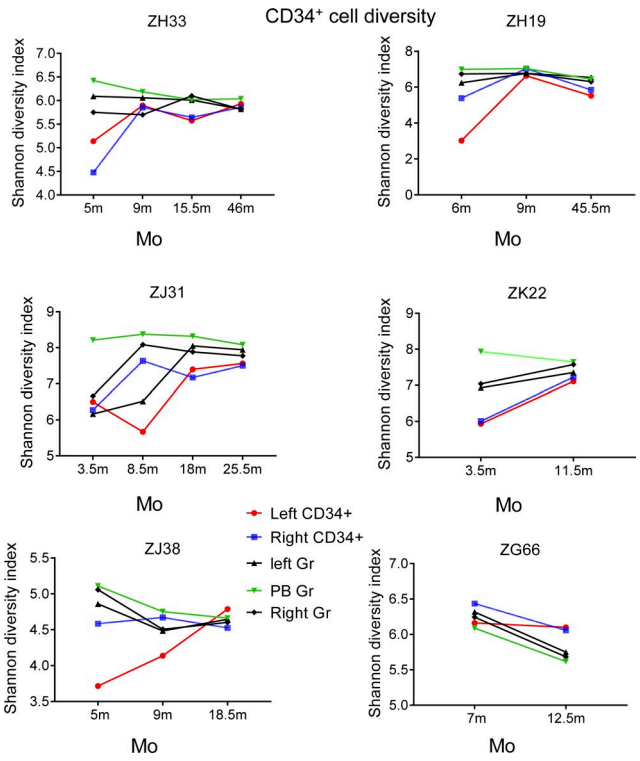

Figure S3. **Clonal diversity of BM CD34⁺ HSPCs and Gr from BM and PB over time after transplantation.** Shannon diversity index of clonal contributions (barcode contributions) retrieved from CD34⁺ HSPCs and Gr from left and right BM samples and PB Gr over time in six animals after transplantation. The Shannon diversity index simultaneously takes into account both the number of clones and their size distribution. For a given number of clones, higher diversity corresponds to a more even distribution of sizes.

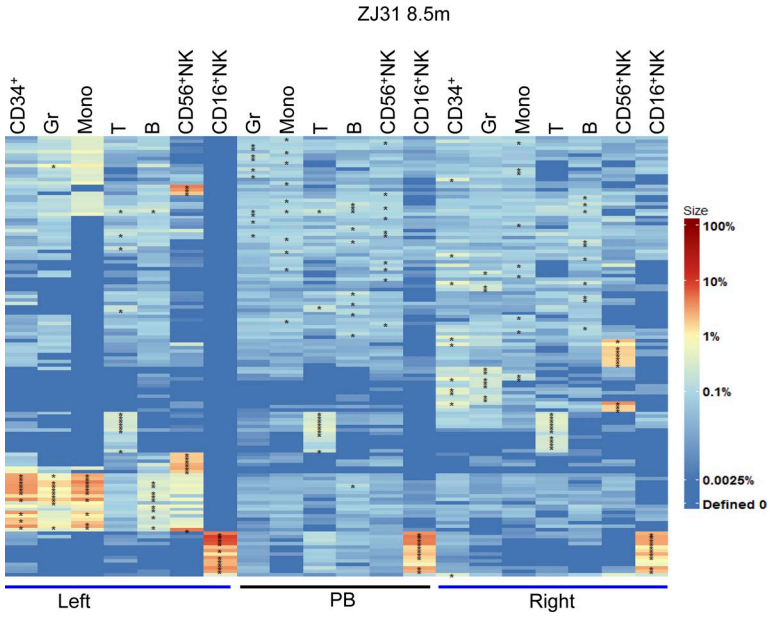

Figure S4. **Clonal heat map of geographic localization of top 10 contributing clones in animal ZJ31 at 8.5 mo.** Heat map representing the log fractional contribution to hematopoiesis of the top 10 most abundant clones in purified $CD34^+$ and Gr, Mono, T, B, and NK cell subsets ($CD56^+$: $CD56^+CD16^-CD3^-CD20^-CD14^-$ NK cells, and $CD16^+$: $CD56^-CD16^+CD3^-CD20^-CD14^-$ NK cells) from left and right BM samples and PB obtained from ZJ31 8.5 mo posttransplantation. m, months.

Table S1. **Antibodies used for flow cytometric sorting of blood, LN, and BM cell populations**

Antigen	Conjugation	Vendor	Catalog number	Clone
CD3	APC-Cy7	BD Pharmingen	557757	SP34-2
CD20	PE-Cy5	BD Pharmingen	555624	2H7
CD14	Pacific blue	Invitrogen	MHCD1428	TUK4
CD16	APC	BioLegend	302012	3G8
CD56	PE	BD Pharmingen	555516	B159
CD56	PE-Cy5.5	Beckman coulter	A79388	N901 (HLDA6)
CD33	PE	Miltenyi Biotec	130-091-732	AC104.3E3
CD34	PE	BD Pharmingen	550761	563
CD34	Purified (for $CD34^+$ selection)	NA	NA	12.8
CD20	APC Cy7	BD Pharmingen	335794	L27
CD4	PE	BD Pharmingen	565999	Sk3
CD8	BUV395	BD Horizon	563795	RPA-T8
CCR5	Percp-Cy5.5	BD Pharmingen	560635	3A9
CD45	Alexa Fluor 647	NA	NA	NA
CD45	BV510	BD Horizon	563830	D058-1283
TCR-αβ	PE	BioLegend	201107	R73
TCR-γδ	BV650	BD Horizon	564156	B1
TCR-Vα24	Percp-Cy5.5	BioLegend	360003	C15/TCR Vα24